



# **Improved Boost Chopper Converter for AC Photovoltaic Module application**

**P.Agaiah<sup>1</sup>, A.V.V. Sudhakar<sup>2</sup>**

PG Student [PE], Dept. of EEE, SR Engineering College, Warangal, Telangana, India<sup>1</sup>

Associate Professor, Dept. of EEE, SR Engineering College, Warangal, Telangana, India<sup>2</sup>

**ABSTRACT:** In photovoltaic (PV) power-generation market, the ac PV module has shown obvious growth. However, a high voltage gain converter is essential for the module's grid connection through a dc–ac inverter. This paper proposes a converter that employs a floating active switch to isolate energy from the PV panel when the ac module is OFF; this particular design protects installers and users from electrical hazards. Without extreme duty ratios and the numerous turns-ratios of a coupled inductor, this converter achieves a high step-up voltage-conversion ratio; the leakage inductor energy of the coupled inductor is efficiently recycled to the load. These features explain the module's high-efficiency performance. The detailed operating principles and steady-state analyses of continuous, discontinuous, and boundary conduction modes are described. A 15V input voltage, 200V output voltage, and 100W output power prototype circuit of the proposed converter has been implemented; its maximum efficiency is up to 95.3% and full-load efficiency is 92.3%.

**KEYWORDS:** AC module, coupled inductor, high step-up voltage gain, single switch.

## **I. INTRODUCTION**

Photovoltaic (PV) power-generation systems are becoming increasingly important and prevalent in distribution generation systems. A conventional centralized PV array is a serial connection of numerous panels to obtain higher dc-link voltage for main electricity through a dc–ac inverter [1]. Unfortunately, once there is a partial shadow on some panels, the system's energy yield becomes significantly reduced [2]. An ac module is a micro inverter configured on the rear bezel of a PV panel [1]–[3]; this alternative solution not only immunizes against the yield loss by shadow effect, but also provides flexible installation options in accordance with the user's budget [4]. Many prior research works have proposed a single-stage dc–ac inverter with fewer components to fit the dimensions of the bezel of the ac module, but their efficiency levels are lower than those of conventional PV inverters. The power capacity range of a single PV panel is about 100W to 300W, and the maximum power point (MPP) voltage range is from 15V to 40V, which will be the input voltage of the ac module; in cases with lower input voltage, it is difficult for the ac module to reach high efficiency [3]. However, employing a high step-up dc–dc converter in the front of the inverter improves power-conversion efficiency and provides a stable dc link to the inverter. When installing the PV generation system during daylight, for safety reasons, the ac module outputs zero voltage [4], [5].

The solar energy through the PV panel and micro inverter to the output terminals are off when switches are OFF. When installation of the ac module is taking place, this potential difference could pose hazards to both the worker and the facilities. A floating active switch is designed to isolate the dc current from the PV panel, for when the ac module is off-grid as well as in the non operating condition. This isolation ensures the operation of the internal components without any residential energy being transferred to the output or input terminals, which could be unsafe.

## **II. PROPOSED METHOD**

The efficiency and voltage gain of the dc–dc boost converter are constrained by either the parasitic effect of the power switches or the reverse recovery issue of the diodes. In addition, the equivalent series resistance (ESR) of the capacitor and the parasitic resistances of the inductor also affect overall efficiency. Use of active clamp technique not only recycles the leakage inductor's energy but also constrains the voltage stress across the active switch, however the tradeoff is higher cost and complex control circuit [1], [6]. By combining active snubber, auxiliary resonant circuit, synchronous rectifiers, or switched-capacitor-based resonant circuits and so on, these techniques made active switch

## International Journal of Advanced Research in Electrical, Electronics and Instrumentation Engineering

(An ISO 3297: 2007 Certified Organization)

**Vol. 4, Issue 11, November 2015**

into zero-voltage switching (ZVS) or zero current switching (ZCS) operation and improved converter efficiency. However, when the leakage-inductor energy from the coupled inductor can be recycled, the voltage stress on the active switch is reduced, which means the coupled inductor employed in combination with the voltage-multiplier or voltage-lift technique successfully accomplishes the goal of higher voltage gain [6].

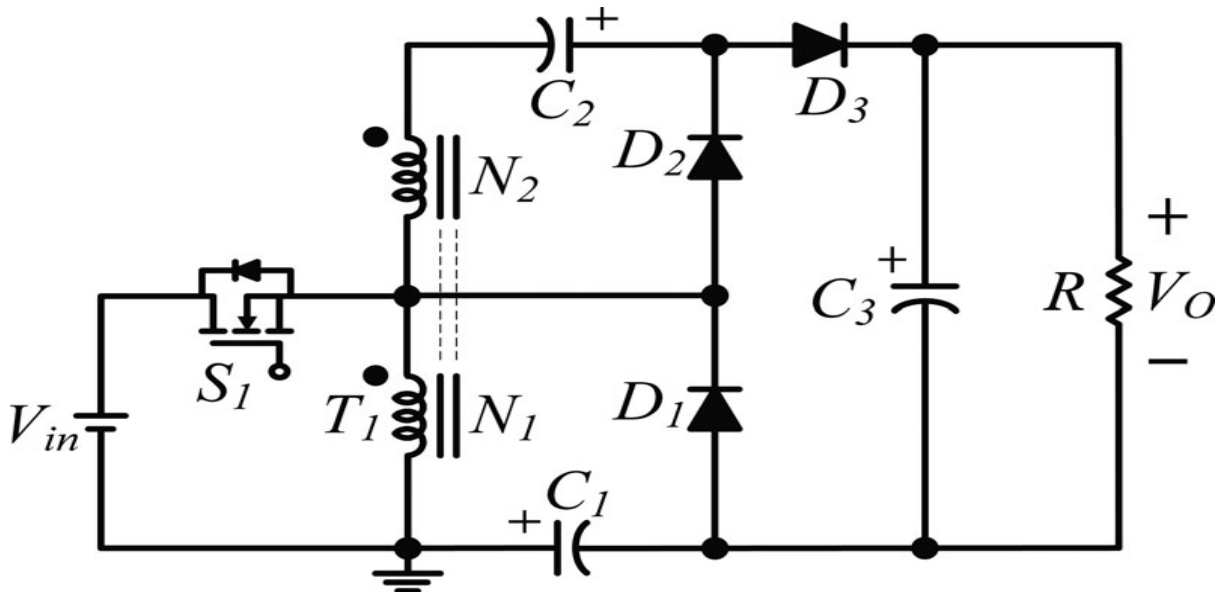


Fig.1 Circuit configuration of proposed converter.

The proposed converter, shown in Fig. 1, is comprised of a coupled inductor  $T1$  with the floating active switch  $S1$ . The primary winding  $N1$  of a coupled inductor  $T1$  is similar to the input inductor of the conventional boost converter, and capacitor  $C1$  and diode  $D1$  receive leakage inductor energy from  $N1$ . The secondary winding  $N2$  of coupled inductor  $T1$  is connected with another pair of capacitors  $C2$  and diode  $D2$ , which are in series with  $N1$  in order to further enlarge the boost voltage. The rectifier diode  $D3$  connects to its output capacitor  $C3$ . The proposed converter has several features: 1) The connection of the two pairs of inductors, capacitor, and diode gives a large step-up voltage-conversion ratio; 2) the leakage-inductor energy of the coupled inductor can be recycled, thus increasing the efficiency and restraining the voltage stress across the active switch; and 3) the floating active switch efficiently isolates the PV panel energy during non operating conditions, which enhances safety. The operating principles and steady-state analysis of the proposed converter are presented in the following sections.

### III. OPERATING PRINCIPLES OF THE PROPOSED CONVERTER

The simplified circuit model of the proposed converter is shown in Fig. 2. The coupled inductor  $T1$  is represented as a magnetizing inductor  $Lm$ , primary and secondary leakage inductors  $Lk1$  and  $Lk2$ , and an ideal transformer. In order to simplify the circuit analysis of the proposed converter, the following assumptions are made.

## International Journal of Advanced Research in Electrical, Electronics and Instrumentation Engineering

(An ISO 3297: 2007 Certified Organization)

Vol. 4, Issue 11, November 2015

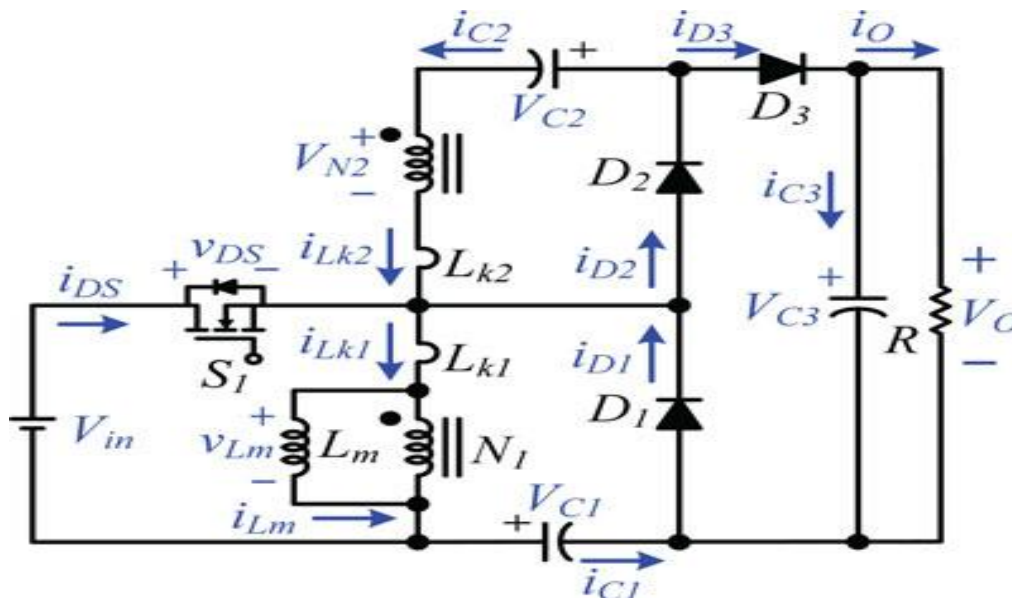


Fig. 2. Polarity definitions of voltage and current in proposed converter.

1) All components are ideal, except for the leakage inductance of coupled inductor  $T1$ , which is being taken under consideration. The on-state resistance  $R_{DS(ON)}$  and all parasitic capacitances of the main switch  $S1$  are neglected, as are the forward voltage drops of diodes  $D1$  and  $D3$ .

2) The capacitors  $C1, C3$  are sufficiently large that the voltages across them are considered to be constant.

3) The ESR of capacitors  $C1, C3$  and the parasitic resistance of coupled inductor  $T1$  are neglected.

4) The turns ratio  $n$  of the coupled inductor  $T1$  windings is equal to  $N2/N1$ .

The operating principle of continuous conduction mode (CCM) is presented in detail. The current waveforms of major components are given in Fig. 4. There are five operating modes in a switching period. The operating modes are described as follows.

### A. CCM Operation:

**Mode I [ $t_0, t_1$ ]:** In this transition interval, the magnetizing inductor  $L_m$  continuously charges capacitor  $C2$  through  $T1$  when  $S1$  is turned ON. The current flow path is shown in Fig. 5(a); switch  $S1$  and diode  $D2$  are conducting. The current  $i_{Lm}$  is decreasing because source voltage  $V_{in}$  crosses magnetizing inductor  $L_m$  and primary leakage inductor  $L_{k1}$ ; magnetizing inductor  $L_m$  is still transferring its energy through coupled inductor  $T1$  to charge switched capacitor  $C2$ , but the energy is decreasing; the charging current  $i_{D2}$  and  $i_{C2}$  are decreasing. The secondary leakage inductor current  $i_{Lk2}$  is declining as equal to  $i_{Lm}/n$ .

Once the increasing  $i_{Lk1}$  equals decreasing  $i_{Lm}$  at  $t = t_1$ , this mode ends.

**Mode II [ $t_1, t_2$ ]:** During this interval, source energy  $V_{in}$  is series connected with  $N2, C1$ , and  $C2$  to charge output capacitor  $C3$  and load  $R$ ; meanwhile magnetizing inductor  $L_m$  is also receiving energy from  $V_{in}$ . The current flow path is shown in Fig. 5(b), where switch  $S1$  remains ON, and only diode  $D3$  is conducting. The  $i_{Lm}, i_{Lk1}$ , and  $i_{D3}$  are increasing because the  $V_{in}$  is crossing  $L_{k1}, L_m$ , and primary winding  $N1$ ;  $L_m$  and  $L_{k1}$  are storing energy from  $V_{in}$ ; meanwhile  $V_{in}$  is also serially connected with secondary winding  $N2$  of coupled inductor  $T1$ , capacitors  $C1$ , and  $C2$ , and then discharges their energy to capacitor  $C3$  and load  $R$ . The  $i_{in}, i_{D3}$  and discharging current  $i_{C1}$  / and  $i_{C2}$  / are increasing. This mode ends when switch  $S1$  is turned OFF at  $t = t_2$ .

**Mode III [ $t_2, t_3$ ]:** During this transition interval, the energy stored in coupled inductor  $T1$  is releasing to  $C1$  and  $C2$ . The current flow path is shown in Fig. 7(c). Only diodes  $D1$  and  $D2$  are conducting. Currents  $i_{Lk1}$  and  $i_{D1}$  are continually decreased because leakage energy still flowing through diode  $D1$  keeps charging capacitor  $C1$ . The  $L_m$  is delivering its energy through  $T1$  and  $D2$  to charge capacitor  $C2$ . The energy

stored in capacitor  $C3$  is constantly discharged to the load  $R$ . These energy transfers result in decreases in  $iLk1$  and  $iLm$  but increases in  $iLk2$ . This mode ends when current  $iLk1$  reaches zero at  $t = t3$ .

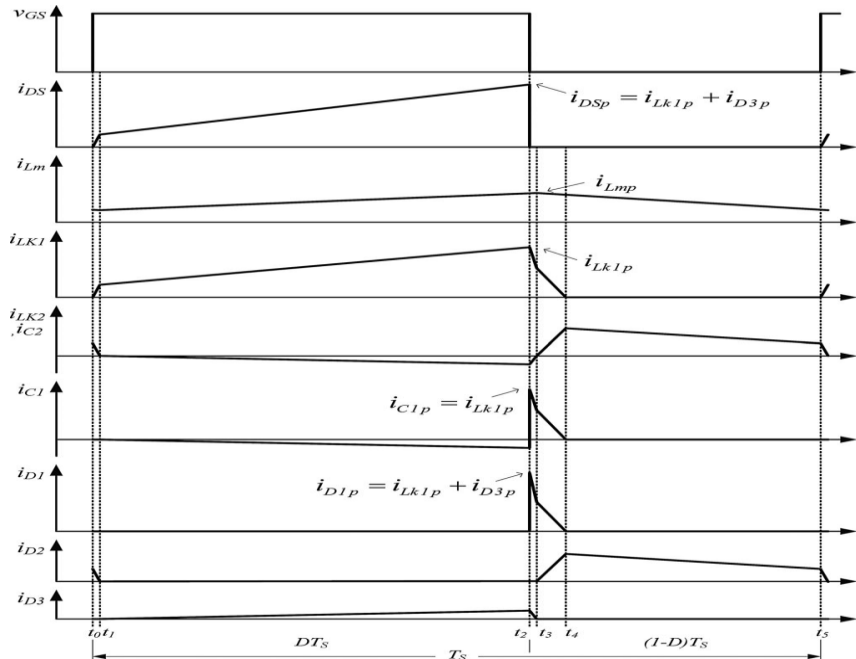


Fig.3. Some typical waveforms of proposed converters at CCM operation.

**Mode IV [ $t3, t4$ ]:** During this transition interval, the energy stored in magnetizing inductor  $Lm$  is released to  $C1$  and  $C2$  simultaneously. The current flow path is shown in Fig. 5(d).

Only diodes  $D1$  and  $D2$  are conducting. Currents  $iLk1$  and  $iD1$  are continually decreased because the leakage energy still flowing through diode  $D1$  keeps charging capacitor  $C1$ . The  $Lm$  is delivering its energy through  $T1$  and  $D2$  to charge capacitor  $C2$ . The energy stored in capacitor  $C3$  is constantly discharged to the load  $R$ . These energy transfers result in decreases in  $iLk1$  and  $iLm$  but increases in  $iLk2$ . This mode ends when current  $iLk1$  is zero, at  $t = t4$ .

**Mode V [ $t4, t5$ ]:** During this interval, only magnetizing inductor  $Lm$  is constantly releasing its energy to  $C2$ . The current flow path is shown in Fig. 5(e), in which only diode  $D2$  is conducting. The  $iLm$  is decreasing due to the magnetizing inductor energy flowing through the coupled inductor  $T1$  to secondary winding  $N2$ , and  $D2$  continues to charge capacitor  $C2$ . The energy stored in capacitor  $C3$  is constantly discharged to the load  $R$ . This mode ends when switch  $S1$  is turned ON at the beginning of the next switching period.

## IV. EXPERIMENTAL RESULTS

A 100W prototype sample is presented to verify the practicability of the proposed converter. The electrical specifications are  $Vin = 15V$ ,  $VO = 200V$ ,  $fS = 50$  kHz, and full-load resistance  $R = 400 \Omega$ . The major components required are  $C1 = C2 = 47 \mu F$  and  $C3 = 220 \mu F$ . The main switch  $S1$  is a MOSFET IXFK180N15P, the diodes  $D1$  are MRB20200CTG, and the DPG30C300HB is selected for  $D2$  and  $D3$ . Since (10) assigns turns ratio  $n = 5$ , the duty ratio  $D$  is derived as 55%. The boundary normalized magnetizing inductor time constant  $\tau LB$  is found by (28) to be  $1.547 \times 10^{-3}$ . To define the proposed converter's BCM operation at 50% of the full load, the load resistance  $R = 800 \Omega$ . The boundary magnetizing inductance

$LmB$  is found as follows:

$$LmB \cdot fSR > 1.547 * 10^{-3} \Rightarrow Lm > 24.75 \mu H.$$

P- sim results

# International Journal of Advanced Research in Electrical, Electronics and Instrumentation Engineering

(An ISO 3297: 2007 Certified Organization)

Vol. 4, Issue 11, November 2015

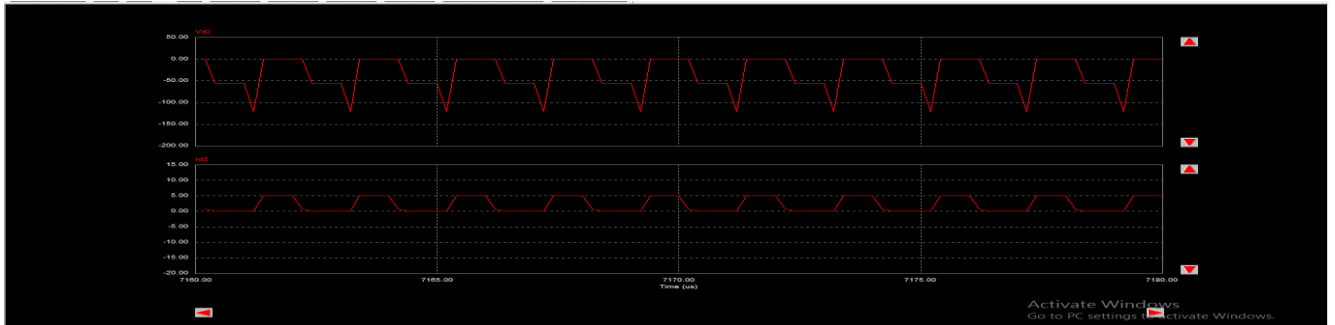


Fig 4.1 Vd2 and Id2

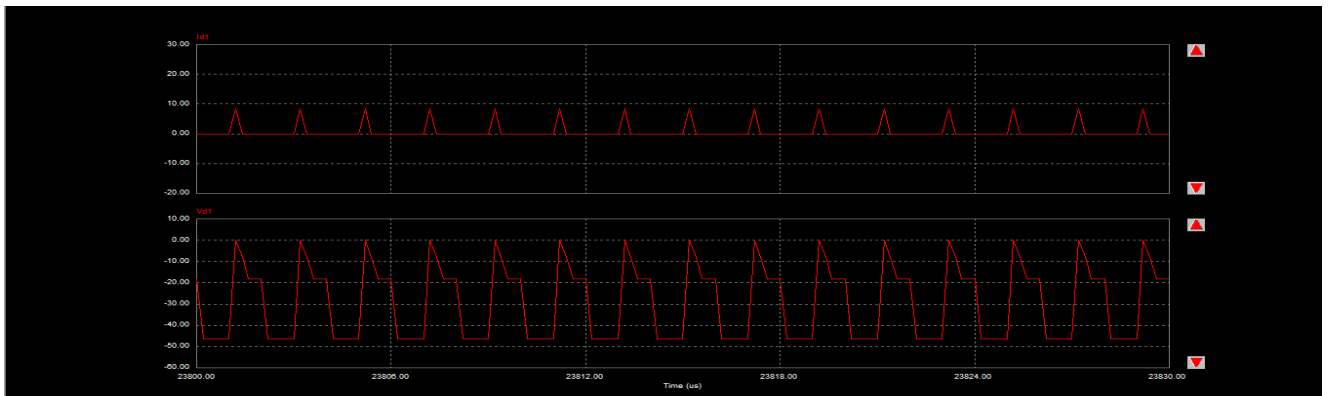


Fig 4.2 Vd1 and Id1

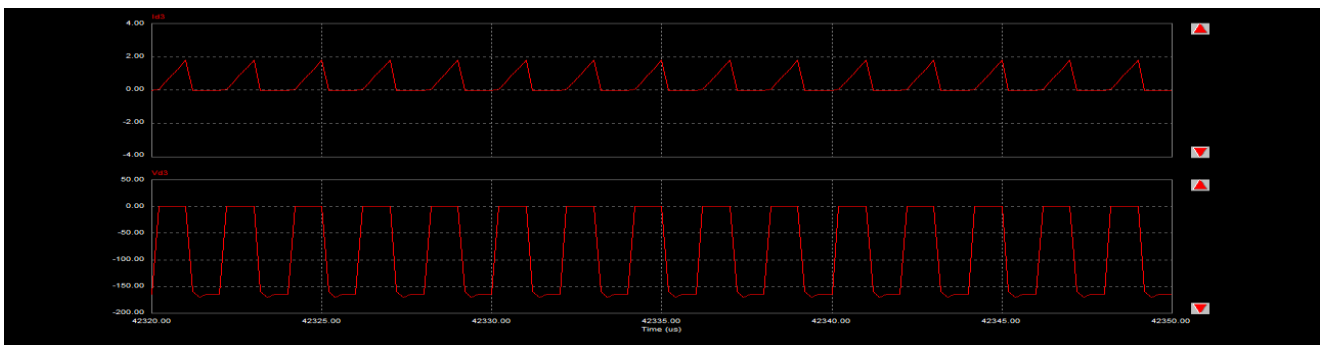


Fig 4.3 vd3 and Id3

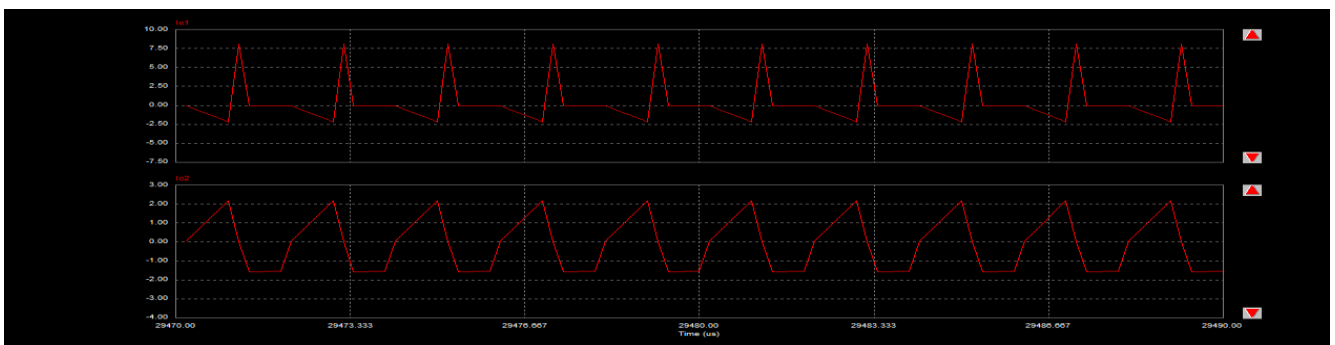


Fig 4.4 Ic1 and Ic2

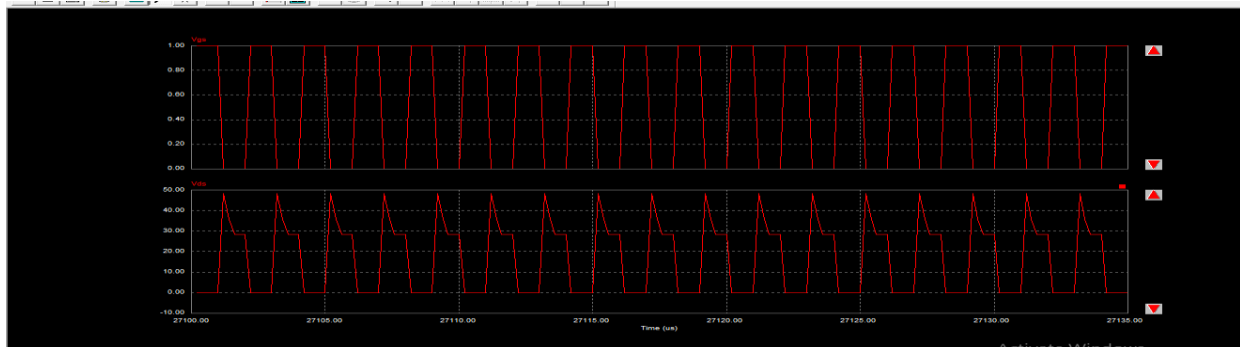


Fig 4.5 Vgs and Vds

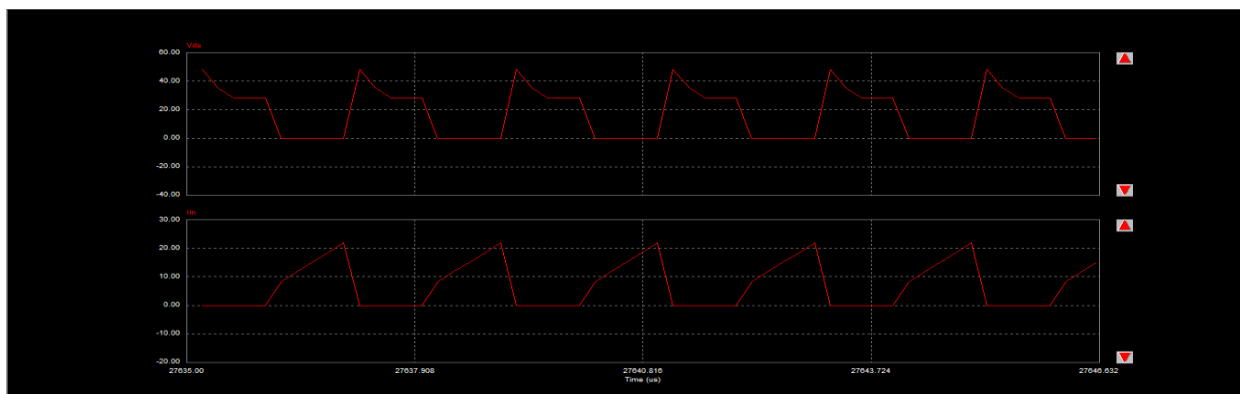


Fig 4.6 Vds and ids

Fig.4. Experimental waveforms measured by the condition of  $f_s = 50$  kHz,  $V_{in} = 15$ V, and output 100W.

## V. CONCLUSION

The energy of the coupled inductor's leakage inductor has been recycled, the voltage stress across the active switch  $S1$  is constrained, which means low ON-state resistance  $R_{DS(ON)}$  can be selected. Thus, improvements to the efficiency of the proposed converter have been achieved. The switching signal action is performed well by the floating switch during system operation; on the other hand, the residual energy is effectively eliminated during the non operating condition, which improves safety to system technicians. From the prototype converter, the turns ratio  $n = 5$  and the duty ratio  $D$  is 55%; thus, without extreme duty ratios and turns ratios, the proposed converter achieves high step-up voltage gain, of up to 13 times the level of input voltage. The experimental results show that the maximum efficiency of 95.3% is measured at half load, and a small efficiency variation will harvest more energy from the PV module during fading sunlight.

## REFERENCES

- [1] T. Shimizu, K. Wada, and N. Nakamura, "Flyback-type single-phase utility interactive inverter with power pulsation decoupling on the dc input for an ac photovoltaic module system," *IEEE Trans. Power Electron.*, vol. 21, no. 5, pp. 1264–1272, Jan. 2006.
- [2] C. Rodriguez and G. A. J. Amaratunga, "Long-lifetime power inverter for photovoltaic ac modules," *IEEE Trans. Ind. Electron.*, vol. 55, no. 7, pp. 2593–2601, Jul. 2008.
- [3] S. B. Kjaer, J. K. Pedersen, and F. Blaabjerg, "A review of single-phase grid-connected inverters for photovoltaic modules," *IEEE Trans. Ind. Appl.*, vol. 41, no. 5, pp. 1292–1306, Sep./Oct. 2005.
- [4] J. J. Bzura, "The ac module: An overview and update on self-contained modular PV systems," in *Proc. IEEE Power Eng. Soc. Gen. Meeting*, Jul. 2010, pp. 1–3.
- [5] B. Jablonska, A. L. Kooijman-van Dijk, H. F. Kaan, M. van Leeuwen, G. T. M. de Boer, and H. H. C. de Moor, "PV-PRIV'E project at ECN, five years of experience with small-scale ac module PV systems," in *Proc. 20th Eur. Photovoltaic Solar Energy Conf.*, Barcelona, Spain, Jun. 2005, pp. 2728–2731.
- [6] T. Umeno, K. Takahashi, F. Ueno, T. Inoue, and I. Oota, "A new approach to low-ripple-noise switching converters on the basis of switched-capacitor converters," in *Proc. IEEE Int. Symp. Circuits Syst.*, Jun. 1991, pp. 1077–1080.